Vortices and confinement at weak coupling

Tamás G. Kovács*
Department of Physics, University of Colorado, Boulder, Colorado 80309-390

E. T. Tomboulis†
Department of Physics, UCLA, Los Angeles, California 90095-1547
(Received 17 November 1997; published 6 March 1998)

We discuss the physical picture of thick vortices as the mechanism responsible for confinement at arbitrarily weak coupling in $SU(2)$ gauge theory. By introducing appropriate variables on the lattice we distinguish between thin, thick and ''hybrid'' vortices, the latter involving $Z(2)$ monopole loop boundaries. We present numerical lattice simulation results that demonstrate that the full $SU(2)$ string tension at weak coupling arises from the presence of vortices linked to the Wilson loop. Conversely, excluding linked vortices eliminates the confining potential. The numerical results are stable under an alternate choice of lattice action as well as a smoothing procedure which removes short distance fluctuations while preserving long distance physics. [S0556-2821(98)02109-2]

PACS number(s): 12.38.Aw, 11.15.Ha, 12.38.Gc

I. INTRODUCTION

Arguments for the presence of spread-out tubes of color-magnetic flux, thick ''vortices,'' being the essential feature responsible for maintaining confinement at arbitrarily weak coupling in $SU(N)$ gauge theory were expounded some time ago [1–6]. A key idea is that such extended structures cost very little action locally, and thus are not directly suppressed at large β. By gradual variation of the gauge fields, they can disorder the vacuum over long scales. The infrared physical picture is, of course, independent of any ultraviolet cutoff details, but, as always with such nonperturbative questions, mathematically precise formulations have been possible only on the lattice. Thick vortices form closed extended structures which are topologically characterized, in the continuum extrapolation, by $\pi_1[SU(N)/Z(N)]=Z(N)$. ''Punctured'' thick vortices, whose (small) ''hole'' boundary is a Dirac monopole current loop, are also possible and survive at large β [6]. (These Dirac monopoles are also classified by the non-trivial elements of $\pi_1[SU(N)/Z(N)]$.) In the $SU(N)$ lattice gauge theory there also occur ''thin'' vortex excitations of the $Z(N)$ part of the group. These are localized to one lattice spacing thickness, and hence are sensitive to the short distance details such as the precise choice of the plaquette action. Long thin vortices are very efficient at disordering the system at strong coupling, but are energetically heavily suppressed and become irrelevant at large β.

In this paper we first discuss in detail the various vortex excitations possible in the $SU(N)$ lattice gauge theory (Sec. II). We treat explicitly the simplest $N=2$ case since no additional physical features appear in the general N extension which is straightforward. The proper distinction between thin and thick vortices and their interactions seems to have occasioned some confusion in the literature. A clean separation can be achieved by an exact rewriting of the $SU(2)$ theory in terms of $SU(2)/Z(2)\sim SO(3)$ and $Z(2)$ variables [3,1]. We eschew any mathematical derivations that can be extracted from the literature, and give a detailed physical discussion of the various excitations and their interactions.[1] In Sec. III we examine the Wilson loop and its interaction with the different types of vortices. In the $SU(2)$ case the fluctuation of the Wilson loops between positive and negative values is *solely* determined by the number (mod 2) of vortices linking with the loop. Namely, if a particular loop in a given configuration is positive/negative, there is an even/odd number of vortices linking with the loop (including all types of vortices). This then allows us to examine the vortex contribution to the string tension numerically (Sec. IV). The string tension extracted from the full Wilson loops was compared to the same quantity extracted from the expectation of only the sign fluctuation counting the linking of the vortices. The computation was first performed with the Wilson action, and then also with a fixed point action in conjunction with a ''smoothing'' procedure based on the renormalization group. The point of performing the comparison also under smoothing is that smoothing removes short distance fluctuations while preserving long distance physics. In particular, the string tension of the full Wilson loop remains unchanged under the smoothing procedure. A necessary test then of any claim concerning the long distance physics is that it remain invariant under the smoothing procedure. The numerical results demonstrate that the confining potential arises from the presence of the vortices linked to the loop: the full string tension is, remarkably, reproduced from the expectation of the vortex counting sign. Conversely, allowing no (mod 2) vortices to link with the loop eliminates the confining potential. Closely related results have been reported in [7]. Our conclusions are presented in Sec. V.

II. VORTICES—THIN, THICK AND HYBRID

For $SU(N)/Z(N)$ gauge fields in the continuum, vortices are topologically classified by $\pi_1[SU(N)/Z(N)]=Z(N)$.

*Email address: kovacs@eotvos.Colorado.EDU
†Email address: tombouli@physics.ucla.edu

[1]This is an extended version of the argument given in [6].

This means that a vortex nontrivially linked to a Wilson loop (trace of the parallel transport matrix of the gauge field connection), taken in the fundamental representation of the covering group $SU(N)$, contributes a factor $z \in Z(N), \quad z \neq 1$. A vortex forms a closed 2-dim surface in $d=4$ (a loop in $d=3$) so that it links with a Wilson loop C if it pierces once any surface bounded by C. Topologically, it is also possible to have gauge field configurations representing ''open'' vortices (Dirac sheets). The boundary of an open 2-dim vortex sheet represents a monopole loop (monopole-antimonopole pair in 3-dim). These are Dirac monopoles, also classified by the non-trivial elements of $\pi_1[SU(N)/Z(N)]$ [8].

Now in the continuum, where the gauge field is an element of the Lie group algebra, there is no local distinction between the pure $SU(N)/Z(N)$ and $SU(N)$ gauge theories. In the lattice formulation, in terms of group element bond variables, of course there is a local distinction. The two differ by the dynamics of the additional $Z(N)$ degrees of freedom present in the $SU(N)$ case. Exciting these Z(N) degrees of freedom on a stack of plaquettes forming a 2-dim closed wall (a closed loop in $d=3$) gives a ''thin'' $Z(N)$ vortex. These are of course the vortices already present in a pure $Z(N)$ lattice gauge theory (LGT). They are ''thin'' because they necessarily have thickness of one lattice spacing. At small β, they are very efficient at disordering the vacuum. At large β, however, they are heavily suppressed by the $SU(N)$ plaquette action, and get progressively frozen out as β increases. Correspondingly, the pure $Z(N)$ LGT gets into a Higgs phase; whereas the distinction between the $SU(N)$ and $SU(N)/Z(N)$ LGT disappears, as it should, as the continuum limit is approached. Thus it is only the *non-Abelian* dynamics of the lattice analogs of the topological $Z(N) = \pi_1[SU(N)/Z(N)]$ vortices, which can, if at all, affect the large β long distance dynamics.

The lattice literature contains many confused or incorrect statements due to failure to properly distinguish between the excitations of the $Z(N)$ part versus the (lattice analogs of the) topological $\pi_1[SU(N)/Z(N)]=Z(N)$ excitations of the $SU(N)/Z(N)$ part of the $SU(N)$ gauge group, and their respective energetics. A formalism that allows one to accomplish such a separation cleanly introduces separate $SU(N)/Z(N)$ and $Z(N)$ variables [3,1]. It is important, of course, that this is done in a gauge-invariant manner, and gives an exact rewriting of the partition function and all observables in terms of the new variables.

From now on we restrict to $SU(2)$, which is the actual case of our numerical simulations below. The extension to any N is straightforward. Consider then the standard $SU(2)$ theory partition function on a lattice Λ,

$$Z_\Lambda = \int \prod_b dU_b \exp\left(\sum_p \beta \mathrm{tr} U_p \right), \tag{1}$$

where, as usual, we wrote $U_p = \Pi_{b \in p} U_b$ for the product of bond variables U_b around the plaquette p.

We now introduce new $Z(2)$ variables $\sigma_p \in \{\pm 1\}$ residing on plaquettes. We write $\sigma_c \equiv \Pi_{p \in c} \sigma_p$ for the product of the σ_p's around the faces of the cube c. We also introduce the coset bond variables $\hat{U}_b \in SU(2)/Z(2) \sim SO(3)$. The configuration space of the the $SU(2)$ bond variables on the lattice Λ is split into equivalence classes, each class corresponding to one coset bond variable configuration $\{\hat{U}_b\}$ on Λ. Thus two $SU(2)$ configurations $\{U_b\}$ and $\{U'_b\}$ on Λ are representatives of the same coset configuration $\{\hat{U}_b\}$ if and only if one has $U'_b = U_b \gamma_b$, for some $\gamma_b \in Z(2)$, for every bond b on Λ. Now given a coset configuration $\{\hat{U}_b\}$, pick a representative $\{U_b\}$ and let $\eta_p \equiv \mathrm{sgn} U_p$. Then the quantity

$$\eta_c(\hat{U}) \equiv \prod_{p \in c} \eta_p, \tag{2}$$

the product of η_p around the faces of a cube c, depends, as indicated, only on the coset variables since it is invariant under $U_b \to U_b \gamma_b$ for $\gamma_b \in Z(2)$. In other words, it is independent of the representative used to compute it.

Now one can show [1,3] that Eq. (1) can be written in the form

$$Z_\Lambda = \int \prod_b dU_b \prod_p d\sigma_p \prod_c \delta[\eta_c \sigma_c] \exp(\beta |\mathrm{tr} U_p| \sigma_p). \tag{3}$$

In Eq. (3), and what follows, the ''delta function'' on $Z(2)$ simply stands for

$$\delta(\tau) \equiv \frac{1}{2}[1+\tau], \quad \tau \in Z(2), \tag{4}$$

so that $\delta(\tau)=1$ for $\tau=1$, $\delta(\tau)=0$ for $\tau=-1$. Also, $\int d\sigma_p(\cdots) \equiv \Sigma_{\sigma_p=\pm 1}(\cdots)$ stands for ''integration'' over the discrete $Z(2)$ group.

The crucial point is that the integrand in Eq. (3) depends only on the $\hat{U}$'s since it is invariant under the local transformation $U_b \to U_b \gamma_b$ for arbitrary $\gamma_b \in Z(2)$. In particular, the action becomes the product of a $Z(2)$ part and an $SO(3)$ part. The $Z(2)$ part, which is given simply by the plaquette variable σ_p, determines the sign of the action. The $SO(3)$ part is non-negative. In this connection note the relation $|\mathrm{tr} U|^2 = |\chi_{1/2}(U)|^2 = 1 + \chi_1(U) = 1 + \chi_1(\hat{U})$, where $\chi_{1/2}(U)$ and $\chi_1(U)$ denote the fundamental and adjoint representation characters of $SU(2)$. Thus the U-integration is in fact a U-integration; i.e., in Eq. (3) one has

$$\prod_b dU_b = \mathrm{const} \times \prod_b d\hat{U}_b, \tag{5}$$

where $d\hat{U}_b$ is the Haar measure over $SO(3)$.

Similarly, for the expectation of a Wilson loop one finds

$$W[C] = \frac{1}{Z_\Lambda} \int \prod_b dU_b \mathrm{tr} U[C] \exp\left(\sum_p \beta \mathrm{tr} U_p \right) \tag{6}$$

$$= \frac{1}{Z_\Lambda} \int \prod_b dU_b \prod_p d\sigma_p \prod_c \times \delta[\eta_c \sigma_c] \mathrm{tr} U[C] \eta_S \sigma_S \exp(\beta |\mathrm{tr} U_p| \sigma_p). \tag{7}$$

In Eq. (7), $U[C] = \Pi_{b \in C} U_b$ stands for the product of the U_b's around the loop C, and we introduced the notations

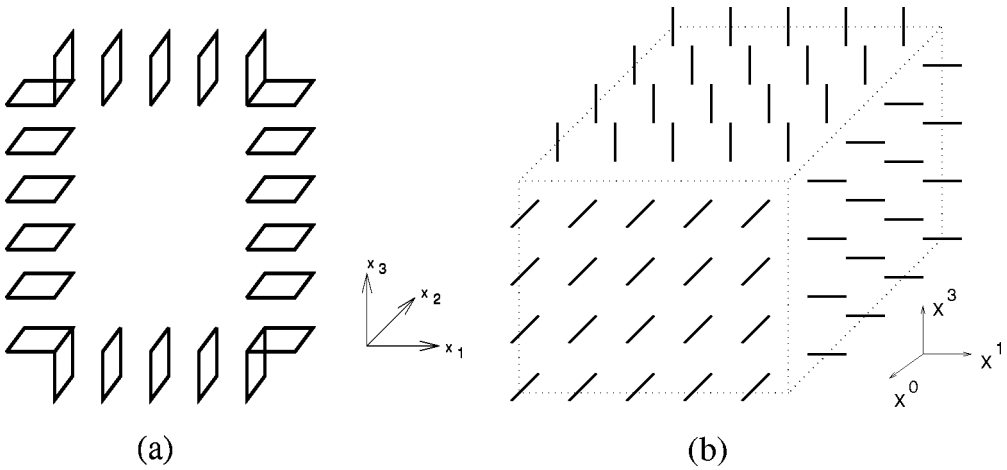

FIG. 1. Thin vortex: (a) $d=3$ or $d=4$ in [123]-section view; (b) $d=4$ in [130]-section 3-dimensional view. Plaquettes protruding in x^2-direction carry $\sigma_p=-1$.

$$\eta_S \equiv \prod_{p\in S} \eta_p\,, \quad \sigma_S \equiv \prod_{p\in S} \sigma_p\,, \tag{8}$$

where S is a surface bounded by the loop C, i.e., $C=\partial S$. It is easily seen that Eq. (7) does not depend on the choice of surface S. Furthermore, the quantity $\mathrm{tr}U[C]\eta_S$ depends only on the $SO(3)$ bond variables $\hat{U}_b$, since it is invariant under $U_b \to U_b\gamma_b$, $\gamma_b \in Z(2)$. The Wilson loop operator is thus expressed as a product of an $SO(3)$ and a $Z(2)$ factor. Similarly, any other observable, such as a 't Hooft loop, or the electric and magnetic flux free-energies can be easily written in terms of the new variables.

Equations (3) and (7) then reexpress the $SU(2)$ LGT as a coupled $SO(3)$-$Z(2)$ theory. This rewriting is exact and gauge invariant. It is very convenient to evaluate all $SO(3)$ quantities in terms of $SU(2)$ representatives,[2] as in Eq. (3), (7). At the risk of being repetitive, let us point out again that, once the passage to the $SO(3)$-$Z(2)$ formalism is made, the quantity $\eta_p=\mathrm{sgn}U_p$ for a representative of a $\{\hat{U}_b\}$ configuration has nothing to do with the sign of the action in the $SU(2)$ formalism (1), (6). This sign, as already noted, is supplanted by the $Z(2)$ variable σ_p. The representative-dependent η_p's can appear in physical quantities only in $SO(3)$ representative-independent combinations, as e.g., Eq. (2). The resulting expressions (3), (7) of the $SO(3)$-$Z(2)$ formulation have a physically rather transparent form exhibiting the presence and manner of coupling of the various possible topological excitations in the LGT (1).

Consider a configuration where $\sigma_p=1$ everywhere except on a stack of plaquettes forming a loop [Fig. 1(a)] where $\sigma_p=-1$. This is a $Z(2)$ vortex in 3 dimensions or a 3-dimensional section of a vortex in 4 dimensions. In $d=4$ there is an extra dimension to move in, so by translation of the loop a vortex forms a 2-dimensional closed surface [Fig. 1(b)]. The short lines in Fig. 1(b) represent a set of bonds. The plaquette protruding in the x^2-direction out of each of these bonds carries $\sigma_p=-1$. A 3-dimensional $[\mu\nu\lambda]=[123]$ section gives then Fig. 1(a). These vortices, generated by the excitations of the $Z(2)$ σ_p variables, are $Z(2)$ ''thin'' vortices, alluded to above. Note that, from Eq. (3), the action cost for exciting such a $Z(2)$ vortex is directly proportional to the area of the vortex sheet.

Consider next opening the thin vortex by breaking the loop of $\sigma=-1$ plaquettes in Fig. 1(a) as depicted in Fig. 2(a). The two cubes at the two ends necessarily satisfy $\sigma_c=-1$. A cube with $\sigma_c=-1$ is the site of a $Z(2)$ monopole, and Fig. 2(a) depicts a monopole-antimonopole pair joined by an open thin vortex, i.e., a string of $\sigma_p=-1$ plaquettes carrying the $Z(2)$ flux. As just noted, there is a direct action cost associated with this σ-string.

Now, because of the $Z(2)$ δ-function constraint in the measure in Eq. (3), a cube with $\sigma_c=-1$ must also have $\eta_c=-1$. A cube for which $\eta_c=-1$ is the site of the lattice analog of a $\pi_1[SO(3)]=Z(2)$ monopole. As pointed out above this statement depends only on the $SO(3)$ coset configuration $\{\hat{U}_b\}$ on the lattice, i.e., the presence or absence of such a monopole on a given cube is a gauge-invariant feature of each $SO(3)$ configuration. Any one representative $\{U_b\}$ of an $SO(3)$ $\{\hat{U}_b\}$ configuration with a monopole on a given cube will necessarily have a string of plaquettes, the Dirac string, beginning at the cube in question, on which $\eta_p=-1$. The string has to end at another monopole cube. Configurations with monopoles that contribute to the partition

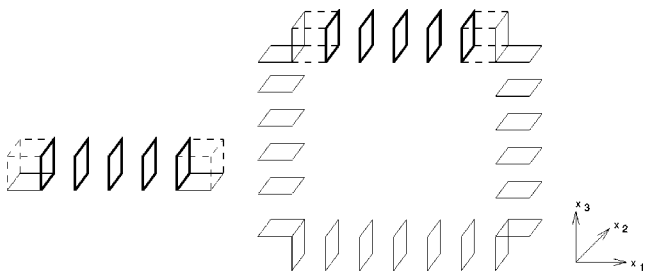

FIG. 2. ($d=3$): (a) $Z(2)$ monopole pair (cubes) joined by σ-string (open thin vortex); (b) the complete configuration including the η-string to form a ''hybrid'' vortex (see text).

[2]They can always, of course, also be expressed directly in (a character expansion in) $SO(3)$ (integer spin) representations, as indicated above for the action plaquette function.

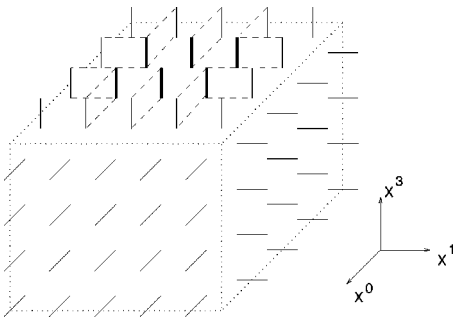

FIG. 3. Hybrid vortex ($d=4$) in 3-dim [130]-section view. Plaquettes protruding in the remaining x^2-direction out of light (heavy) bonds carry $\eta_p=-1(\sigma_p=-1)$; the boundary between the light and heavy sets is a $Z(2)$ monopole current loop (see text).

function then are of the form depicted in Fig. 2(b) in 3 dimensions; heavy plaquettes carry $\sigma_p=-1$, light plaquettes carry $\eta_p=-1$. Note that the location and shape of the string (light plaquettes) depends on the choice of representative; it can differ for different representatives of the same $\{\hat{U}_b\}$ configuration since it may be moved around at will, as a Dirac string should, by letting $U_b\rightarrow\gamma_b U_b$, $\gamma_b\in Z(2)$, i.e., change of representative. The η-string is then ''invisible'' to the $\{\hat{U}_b\}$ configuration on Λ, and hence to the measure, and in particular to the action in Eqs. (3), (7). There is no cost in action associated with the location of the Dirac η-string.

In $d=4$ the monopoles, i.e., the set of cubes on which $\eta_c=-1$, form closed monopole current loops reflecting magnetic current conservation. This follows directly from the definition of the quantity[3] η_c, Eq. (2). A string then sweeps out a Dirac sheet bounded by the corresponding monopole loop. So in $d=4$ the configuration in Fig. 2(b) gives rise to a 'hybrid' vortex forming a closed 2-dimensional surface as shown in Fig. 3. Here again, $\sigma_p=-1$ on the plaquette protruding in the x^2-direction out of every heavy bond, whereas $\eta_p=-1$ on the plaquette protruding in the x^2-direction out of every light bond shown. The plaquettes containing both a light and a heavy bond in their boundary are also shown in the figure. The cube protruding in the x^2-direction out of each of these plaquettes then has $\sigma_c=\eta_c=-1$. This set of cubes forms the monopole current loop (cf. footnote 3). A [123]-section view of Fig. 3 gives then Fig. 2(b). Such a hybrid vortex may be viewed as put together by joining an ''open'' $\pi_1[SO(3)]$ vortex plaquette sheet and an open $Z(2)$ vortex plaquette sheet along their respective monopole loop boundaries. These boundaries must coincide, as noted above, because open vortices as in Fig. 2(a) cannot exist due to the constraint in the measure in Eq. (3).

[3]Indeed it follows from Eq. (2) that η_c obeys the identity

$$\prod_{c\in h}\eta_c=1,$$

where the product is over all cubes c forming the boundary of the elementary hypercube h. Geometrically, this means that the cubes on which $\eta_c=-1$ form closed sets on the dual lattice. In $d=4$, a cube is dual to a bond, so the cubes form closed loops of dual bonds.

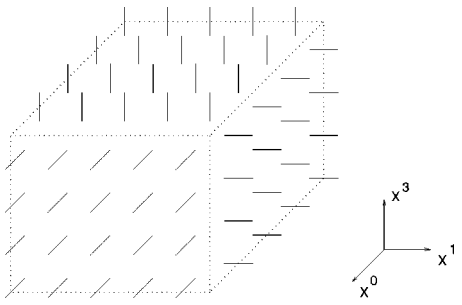

FIG. 4. Thick vortex closed Dirac sheet ($d=4$) in 3-dim [013]-section view; plaquettes protruding in the remaining x^2-direction carry $\eta_p=-1$.

Closed Dirac plaquette sheets form the lattice analogs of $\pi_1[SO(3)]$ vortices (Fig. 4), the set of plaquettes with $\eta_p=-1$ being stacked over a closed 2-dimensional surface (a loop in $d=3$). In the illustration of Fig. 4 each plaquette carrying $\eta_p=-1$ protrudes in the x^2-direction out of the set of bonds shown distributed over a 2-dimensional surface placed in a 3-dimensional [013]-section. Again, the precise location and shape of this $\eta_p=-1$ set of plaquettes forming the Dirac sheet is irrelevant, it being ''invisible'' in the measure (3). What is relevant is only the coset configuration $\{\hat{U}_b\}$ describing the vortex; an $SU(2)$ representative $\{U_b\}$ of such a coset configuration will then contain somewhere on Λ a Dirac sheet, which may be moved around at will by a change of representatives. (Equivalently, the presence of the vortex can be characterized in terms of the $\hat{U}_b$'s only—see below.) Note that, since $Z(2)$ [or generally $Z(N)$] flux is conserved only mod2(mod$N$), this implies that a vortex such as in Fig. 4 is ''unstable'' unless it is topologically nontrivial with respect to the lattice Λ or an externally introduced source in Λ, such as a Wilson loop. Indeed, by a change of representatives, the sheet may always be collapsed to a point annihilating the $Z(2)$ flux, unless there is a topological obstruction. Thus on a lattice with periodic boundary conditions, i.e., the topology of the torus, a vortex as in Fig. 4 may become topologically stable by wrapping completely around the lattice in the x^3,x^0-directions as shown schematically in Fig. 5(a). Here, short light lines represent a Dirac sheet of $\eta_p=-1$ plaquettes, each in a [12]-plane, stacked along the x^3,x^0-directions around the periodic lattice. Such a topologically nontrivial closed sheet can be moved or distorted by a change representative, but not removed. Every representative

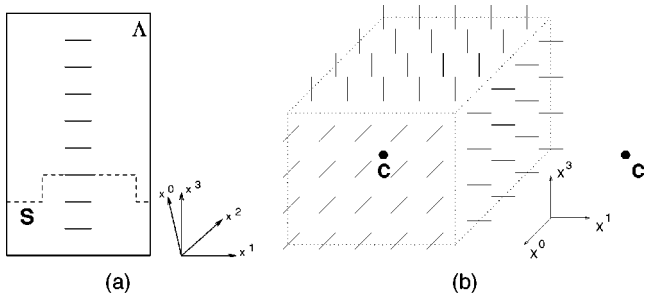

FIG. 5. (a) Topologically nontrivial vortex sheet (short lines) winding around periodic lattice (b) Vortex linked with Wilson loop C; 3-dimensional [130]-section view, with C lying in the [12]-plane.

of the relevant $\{\hat{U}_b\}$ vortex configuration has then an irremovable sheet of $\eta_p=-1$ plaquettes signaling the trapped $Z(2)$ flux of a (an odd number of) topologically nontrivial vortex (vortices). A characterization directly in terms of the $\hat{U}_b$'s is given by the quantity η_S defined as in Eq. (8) but with S now any closed topologically nontrivial surface winding around the lattice in the x^1,x^2-directions [dashed line in Fig. 5(a)]. Then, clearly, η_S is only a function of the cosets $\{\hat{U}_b\}$, and $\eta_S(\hat{U})=-1(+1)$ signifies the presence of an odd (even) number of vortices winding around the lattice in the x^3,x^0-directions normal to S. An analogous description applies to $\pi_1[SO(3)]$ vortices nontrivially linked with the Wilson loop [Fig. 5(b)] discussed below.

As already noted, the $Z(2)$ thin vortices are necessarily localized in thickness to one lattice spacing, and have a direct action cost proportional to their area (length in $d=3$) along which $\sigma_p=-1$. Long thin vortices are then heavily suppressed at large β as the σ $Z(2)$ variables are progressively frozen out. Indeed, it can be shown that the probability of exciting $\sigma_p=-1$ on a plaquette is exponentially suppressed with large[4] β. Only short thin vortices remain then with (exponentially in β) small probability. This probability can actually depend on the choice of the lattice action.[5] This dependence on the short distance structure is, of course, precisely a statement of the fact that thin vortices are thin.

In contrast, the (lattice analog of the) $\pi_1[SO(3)]$ vortices are not necessarily localized, and do not have a direct action cost proportional to their sheet area. Indeed, smooth $\{\hat{U}_b\}$ vortex configurations are easily constructed such that the local plaquette action cost can be made arbitrarily small by making the vortex sufficiently spread out [2,3]. Any $SU(2)$ representative $\{U_b\}$ of the $\{\hat{U}_b\}$ configuration for such a spread-out vortex will of course have a Dirac sheet plaquette set on which $\eta_p=-1$, as discussed above, while $\eta_p=1$ everywhere else; but in such a manner that one still has $|\mathrm{tr}U_p|\simeq 1$ everywhere. The exact location of the Dirac sheet is in fact irrelevant since it can be moved by changing the representative, which does not affect $|\mathrm{tr}U_p|$. The point is, of course, that the action depends only on $|\mathrm{tr}U_p|$, i.e., $\{\hat{U}_b\}$. These ''thick'' vortices are thus not directly suppressed at large β. In fact, long thick vortices winding around the lattice or a large Wilson loop can exist at arbitrarily weak coupling by being sufficiently thick in the directions transverse to their (topologically nontrivially linked) Dirac sheet. The same holds true for long hybrid vortices with a long thick vortex section, and a short (say, one plaquette long) thin vortex section appearing as a localized ''defect'' incurring only a local cost in action [3,6]. These long hybrid vortices may be simply viewed as ''punctured'' thick vortices, the size of the ''hole,'' where the σ_p $Z(2)$ variables are excited, being suppressed, hence small at large β.

Such very long thick vortices (whole or punctured) can then have a very disordering long-distance effect at weak coupling as the bond variables $\hat{U}_b$, over sufficiently large scales, vary smoothly over large parts of the $SU(2)/Z(2)$ group with very little local action cost. Their presence appears in fact to be the necessary condition for confinement at weak coupling, as we discuss in the next section.

It is also interesting to view thick vortices in the d-dimensional theory from a $(d-1)+1$-dimensional perspective by singling out the ''time'' direction [3]. The d-dim gauge theory may be viewed [in Kaluza-Klein (KK) fashion] as a $(d-1)$-dim gauge theory coupled to a Higgs field. A thick vortex may then be viewed within a $(d-1)$-dim slice as a ''monopole''-''antimonopole'' pair. Here the ''monopole'' has *two* units (mod 2) of flux (and hence two η-strings emanating from it), since it may be considered as put together out of two of our $Z(2)$-monopoles and is trivial under $\pi_1[SO(3)]$. Within a given $(d-1)$-dim slice, however, it may be characterized by using the ''Higgs'' field of the KK dimensional reduction to define a homotopy $\pi_2[SO(3)/U(1)]$ group. These ''monopoles'' appear then as lattice analogs of the 't Hooft–Polyakov monopole in $(d-1)$ dimensions. In an appropriate gauge these correspond to the ''monopoles'' of the Abelian projection. This is, of course, not a fundamental, gauge invariant description of the physical picture which is that of the $\pi_1[SO(3)]$ vortices. Still, it may be used as a basis for an approximate computational scheme for obtaining some estimate on the Wilson loop at weak coupling [3]. Some numerical investigation of this picture has recently been reported in [7].

III. THE WILSON LOOP AND VORTICES

Having identified the various types of vortices that occur in the $SU(2)$ LGT, the expression (7) for the Wilson loop is seen to have a rather transparent physical meaning. It makes explicit the interaction of the loop with vortices. Let us write Eq. (7) succinctly as

$$W[C]=\langle \mathrm{tr}U[C]\,\eta_S\sigma_S\rangle_{SO(3)\cup Z(2)}, \tag{9}$$

where the expectation on the right-hand side is taken in the measure (3). As noted above, Eq. (9) decomposes the Wilson loop operator into a $Z(2)$ part σ_S and an $SO(3)$ part $\mathrm{tr}U[C]\,\eta_S=|\mathrm{tr}U[C]|\mathrm{sgn}(\mathrm{tr}U[C]\,\eta_S)$. It is crucial that the expectation (9) does not depend on the choice of the surface S spanning the loop. Then, for a given $\{\{\hat{U}_b\},\{\sigma_p\}\}$ configuration on the lattice:

If $\sigma_S=-1$ for *every* choice of the spanning surface S, a thin vortex, or an odd number of thin vortices, is nontrivially linked with the loop C [Fig. 6(a)]. Conversely, $\sigma_S=1$ for every S signifies an even number (including zero) of thin vortices linked with C.

If $\mathrm{sgn}(\mathrm{tr}U[C]\,\eta_S)=-1$ for *every* choice of the spanning surface S, a thick vortex, or an odd number of thick vortices, is nontrivially linked with the loop C [Fig. 6(b)]. Conversely, $\mathrm{sgn}(\mathrm{tr}U[C]\,\eta_S)=1$ for every S signifies an even number (including zero) of thick vortices linked with C.

[4]This is proven nonperturbatively by ''chessboard estimates'' [9].

[5]Thus the density of the thin $Z(2)$ vortices, and/or $Z(2)$ monopoles, may be enhanced or further suppressed by various short-distance modifications of the original lattice (Wilson) action in Eq. (1). Common modifications in the literature involve the addition of chemical potentials, the MP and the ''positive plaquette'' models, and models introducing new $Z(2)$ degrees of freedom in addition to the σ_p's.

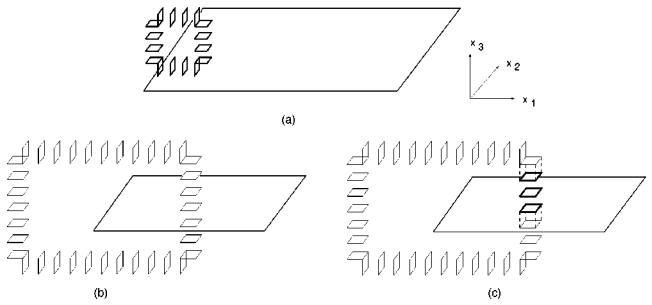

FIG. 6. Wilson loop linked with (a) thin vortex, (b) thick vortex, (c) hybrid vortex; 3-dimensional [123]-section view [cf. Fig. 5(b)].

If neither $\sigma_S=-1$, nor $\mathrm{sgn}(\mathrm{tr}U[C]\eta_S)=-1$ for *every* choice of S, but $\sigma_S\mathrm{sgn}(\mathrm{tr}U[C]\eta_S)=-1$ for *every* choice of S, a hybrid vortex, or an odd number of hybrid vortices, is nontrivially linked with C [Fig. 6(c)]. Conversely, $\sigma_S\mathrm{sgn}(\mathrm{tr}U[C]\eta_S)=1$ for every S signifies that an even number (including zero) of hybrid vortices is linked with C.

Thus the passage to the variables $\hat{U}_b,\sigma_p$ exhibits the Wilson operator explicitly as a vortex counter. The fluctuation of the operator between positive and negative values is entirely due to the presence of vortices linking with the loop. The expectation of this fluctuation is what essentially determines then the behavior of the Wilson loop.

The physically inessential $|\mathrm{tr}U[C]|$, which contributes only a perimeter effect, can in fact be eliminated from expression (7) by switching from the Wilson loop to the electric-flux free energy order parameter F_{el} [10] defined on a lattice with periodic boundary conditions in all directions ($\Lambda=T^d$). Expressed in our variables (3), the electric-flux free energy is given simply by:

$$\exp(-F_{el})=\langle\eta_S\sigma_S\rangle_{SO(3)\cup Z(2)}, \tag{10}$$

where S is any 2-dimensional closed topologically nontrivial surface winding around the lattice in two given directions as in Fig. 5. (The expectation does not depend on the specific choice of S.) By the above enumeration, Eq. (10) shows that the electric-flux free-energy operator is *nothing but* a vortex counter for the various types of vortices winding around the lattice (in the directions perpendicular to S).

Let us return to the consideration of the Wilson loop expectation (9). At large β, long thin vortices, having large vortex sheet area A, disappear as they incur an action cost proportional to βA. Only a dilute gas of short thin vortices remains. For a large Wilson loop, short vortices can link with it only along the loop perimeter [as depicted for the thin vortex in Fig. 6(a)]. At large β, therefore, thin vortices can only contribute at most to a length-law piece in the expectation (7). This in fact can be proven rigorously; it is equivalent to the statement that a pure $Z(2)$ theory is in a Higgs phase at large β.

Long thick vortices, on the other hand, are not directly suppressed by the action at large β. They may therefore link with a large loop anywhere over the area enclosed by the loop [as in Fig. 6(b)]. This may then lead to area-law behavior for the expectation, provided that the class of thick vortex configurations contributes at large β with a finite measure in the path integral sum. The same holds for long hybrid vortices, i.e., long thick vortices ''punctured'' by a small monopole loop forming the boundary of a short thin vortex segment [Fig. 6(c)]. Indeed, long $Z(2)$ monopole loops are spanned by correspondingly large thin vortex sheets and suppressed at large β; but a dilute gas of short monopole loops survives at any finite β. [The shortest possible loop is due to the excitation of $\sigma_p=-1$ on a single plaquette p, forming a one-plaquette-long thin segment, and giving a $Z(2)$ monopole loop consisting of the $2(d-2)$ cubes sharing this p on their boundary and hence having $\sigma_c=-1$.] In the absence of an artificial suppression of negative plaquettes (imposed, for example, by some modification of the action), this dilute gas of short Z(2) monopole loops can be used to tag hybrid vortices and estimate their contribution to the Wilson loop [6].

One may modify the theory to exclude all $Z(2)$ monopoles and hence all hybrid vortices by inserting in the measure (3) the constraint

$$\prod_c \delta[\sigma_c]. \tag{11}$$

This is the Mack-Petkova (MP) model[6] [1]. Confinement at large β in the MP model must then come from the thick vortices. Alternatively, one may instead eliminate all thick closed vortices linking with a given Wilson loop by inserting in the measure in the expectation (9) the constraint

$$\theta[\mathrm{tr}U[C]\eta_S], \tag{12}$$

for any one particular surface S spanning the loop. Similarly, thick vortices winding around a periodic lattice may be excluded from the theory by inserting the constraint

$$\delta[\eta_S], \tag{13}$$

for any particular closed topologically nontrivial surface S running through the lattice in two given directions [cf. Fig. 5(a)]: Eq. (13) eliminates all vortices winding in the $(d-2)$ directions normal to S. In the presence of the constraints (12) or (13), confining behavior for Eqs. (9) or (10), respectively, at large β can then come only from the hybrid vortices. This is the approach taken in [6].

Consider now inserting *both* the constraints (11) and (12), respectively Eq. (13) in the measure, thus eliminating both all hybrid vortices *and* all thick vortices winding through the Wilson loop, respectively the lattice. The form of the expectation (9), respectively Eq. (10), now immediately suggests that confining behavior at large β is lost, i.e., that *the presence of thick or hybrid vortices is the necessary condition for confinement to occur at weak coupling.* In the case of the electric-flux free energy, Eq. (10), a mathematically rigorous

[6]Note that the solution to the constraint (11), which is equivalent to requiring $\eta_c=1$ on all cubes, is given by

$$\sigma_p=\prod_{b\in p}\gamma_b,$$

where γ_b are $Z(2)$ bond variables, i.e., the $Z(2)$ system in Eq. (3) becomes exactly a (Wilson) $Z(2)$ LGT. This is as one would expect: in the absence of $Z(2)$ monopoles, only closed thin vortices are allowed as excitations of the σ_p's, which is the case in a pure $Z(2)$ LGT.

proof of this fact was given in [2] some time ago. The physical implications of this result for discussions of ''mechanisms of confinement'' appears not to have been widely appreciated. It would clearly be important to have the corresponding proof for the case of the Wilson loop.[7] Unfortunately, the proof in [2] does not immediately extend to the Wilson loop case. We will address this question elsewhere.

IV. VORTEX CONTRIBUTION TO HEAVY-QUARK POTENTIAL—NUMERICAL RESULTS

As we saw in the previous section, the sign fluctuation of the Wilson loop operator is determined by its interaction with vortices; a negative Wilson loop signals an odd number of vortices (including all types) linking with the loop. (In fact, in the case of the electric-flux free-energy, this interaction sign constitutes the entire operator.) This then allows one to directly examine the vortex contribution to the Wilson loop. We simply replace the value of the Wilson loop operator by its sign and consider the expectation

$$E[C]\equiv\langle \mathrm{sgn}(\mathrm{tr}U[C])\rangle=\langle \mathrm{sgn}(\mathrm{tr}U[C]\,\eta_S)\sigma_S\rangle_{SO(3)\cup Z(2)}. \tag{14}$$

The expectation (14) is the vortex count expectation value as discussed above. $E[C]$ counts all types of vortices together and can be simply evaluated by the usual Monte Carlo technique in terms of the original $SU(2)$ bond variables. In the following we wish to compare the string tension extracted from the full Wilson loop expectations [Eqs. (6) and (7)] with the string tension obtained from the expectation of the sign of the Wilson loops defined by Eq. (14).

In all our measurements we extracted the heavy quark potential from timelike Wilson loops using the method and the code of Ref. [12]. We computed both on-axis and off-axis loops and the effective potential for different time extensions T was obtained as

$$V(R,T)=-\ln\frac{W(R,T+1)}{W(R,T)}. \tag{15}$$

In principle the heavy quark potential is the $T\to\infty$ limit of $V(R,T)$. In the following we always display the effective potential for a time extent where it has already reached a good plateau. Typically with our values of the coupling this already happens when T equals a few lattice spacings.

At first we used two ensembles of configurations generated with the Wilson action at $\beta=2.4$ and 2.5 where the lattice spacing is $a=0.12$ fm and 0.085 fm respectively. Our results are presented in Figs. 7 and 8. It is striking that the full Wilson loops and just their signs — the vortex expectations — give exactly the same heavy quark potential including the short-distance behavior and even the constant. We emphasize that we have not even shifted the two potentials by a constant; Figs. 7 and 8 show the ''raw'' data without any further manipulation.

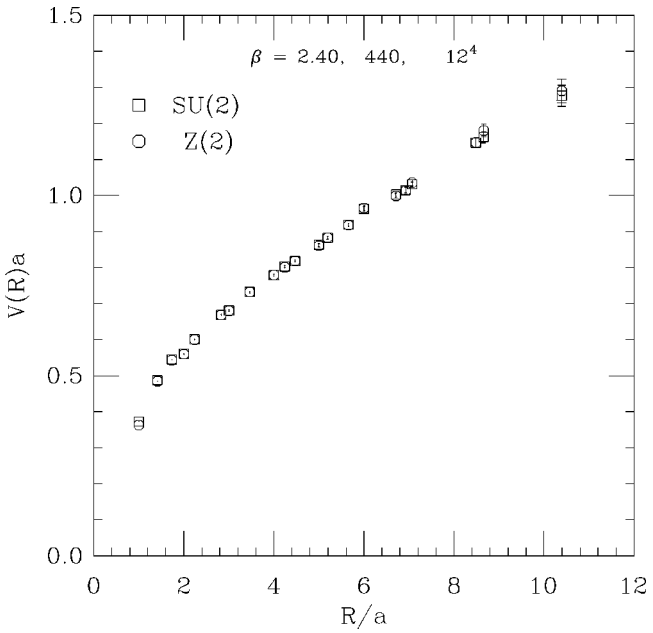

FIG. 7. The heavy quark potential measured on an ensemble of 440 12^4 configurations generated at Wilson $\beta=2.4$. Squares represent the potential obtained from Wilson loop averages, the octagons come from the sign averages.

The remarkable coincidence of the potentials computed in this way shows that the sign of the Wilson loop, i.e., the number of vortices (mod 2) linking with it, contains all the

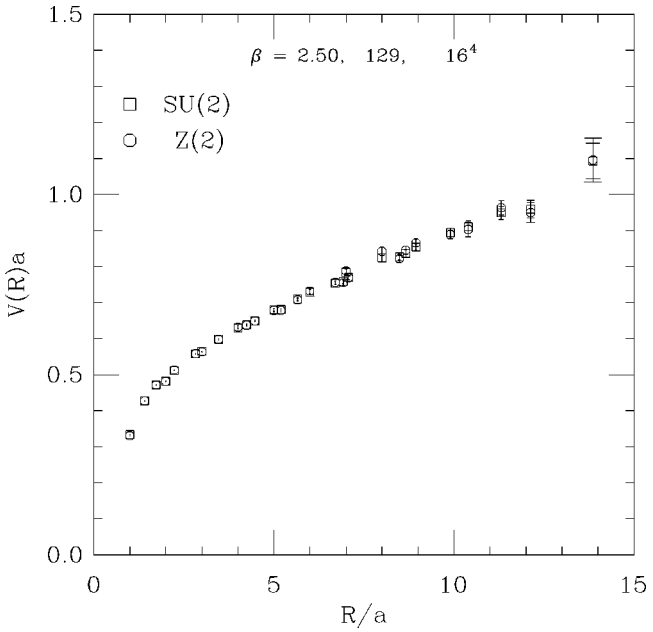

FIG. 8. The heavy quark potential measured on an ensemble of 129 16^4 configurations generated at Wilson $\beta=2.5$. Squares represent the potential obtained from Wilson loop averages, the octagons come from the sign averages.

[7]Asymptotically large Wilson loops are physically essentially equivalent to the electric-flux free energy order parameter. In general, however, the string tension derived from the electric-flux free energy has only been rigorously shown to form a lower bound on the Wilson loop string tension [11]. Thus confining behavior for F_{el} implies confining behavior for the Wilson loop, but not, necessarily, the converse. In any case, as F_{el} is an order parameter that refers to the entire lattice, it is important to obtain the proof corresponding to the result in [2] also for a large but finite Wilson loop as the lattice is taken to the thermodynamic limit.

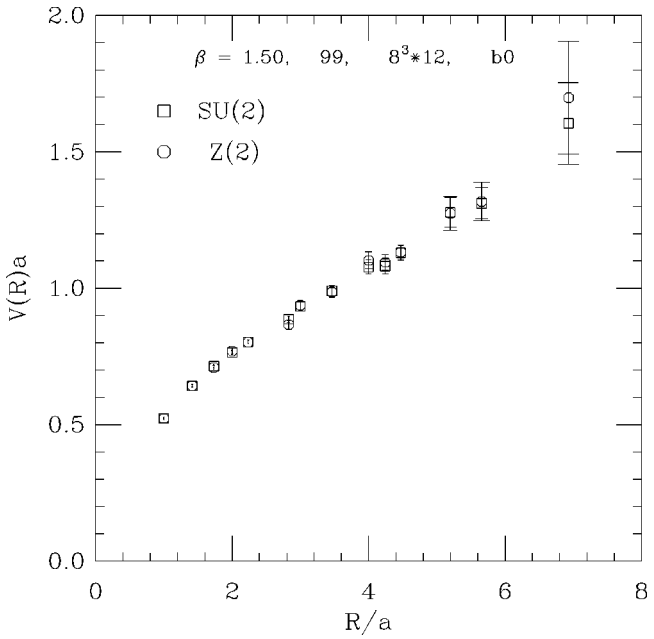

FIG. 9. The heavy quark potential measured on an ensemble of 100 $8^3\times 12$ configurations generated with a fixed point action (lattice spacing $a=0.14$ fm). Squares represent the potential obtained from Wilson loop averages, the octagons come from the sign averages.

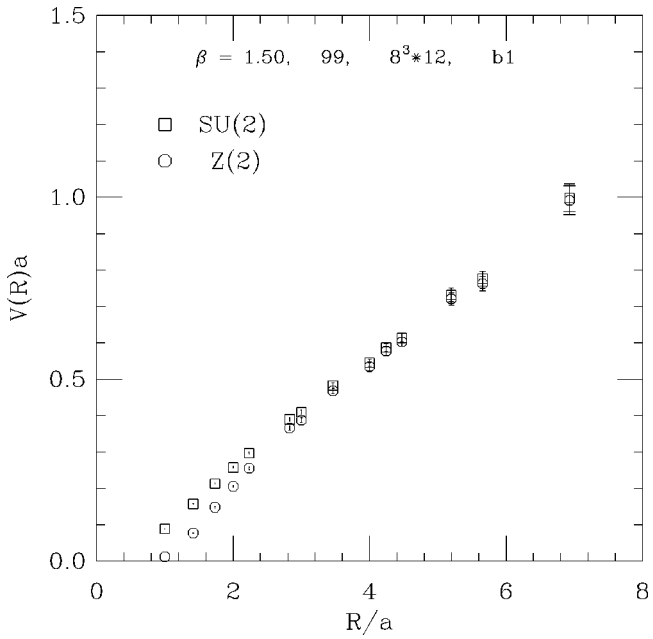

FIG. 10. The heavy quark potential on the same ensemble as Fig. 9 but measured after one smoothing step. Squares represent the potential obtained from Wilson loop averages, the octagons come from the sign averages.

important physics. The short-distance agreement of the potentials can be explained by noting that the sign expectation contains *all* the vortices including thick ones (η) and thin ones (σ). The latter are important at short distances. Furthermore, as we saw in the previous section, thin vortices affect the perimeter-law term in the Wilson loop of any size. This in turn contributes to the constant term in the potential. The fact that even this constant is the same for the two potentials also shows that they contain the same contribution from thin vortices.

At this point one could ask how robust this picture is, in particular how sensitive it is to the physically unimportant short distance details of the configurations. This can be checked either by modifying the action or by taking the Monte Carlo generated configurations and performing some local smoothing on them which does not change the long-distance physical features. If the potential extracted from the sign of the Wilson loops is really equivalent to the full potential then their agreement at long distances should persist on the modified configurations. This is a very stringent test which has already been performed in the case of Abelian dominance. There it turned out that while on the original configurations the Abelian string tension agreed with the full $SU(2)$ string tension to within 8%, after smoothing the difference increased to about 30% [13]. Similar results have been obtained with cooling in Ref. [14]. In the present case at first we repeated the measurement of the full and ''sign'' potentials using the fixed point action of Ref. [15] at lattice spacing $a=0.14$ fm. The results presented in Fig. 9 are very similar to the Wilson data; there is no measurable difference between the potentials. We then performed one step of local smoothing on the same ensemble of configurations. This was done by the renormalization group based smoothing introduced in Ref. [15]. This local smoothing was designed to smooth only on the shortest distance scale, leaving all the long-distance physical features — most notably the string tension — unchanged. On the smoothed configurations the two potentials were measured again. Comparing the potentials obtained on the smoothed configurations (Fig. 10) one can see that for distances $R\geqslant 2$ (in lattice units) they agree but for $R\leqslant 2$ the potential obtained from the signs is systematically below the full potential. This means that the smooth-

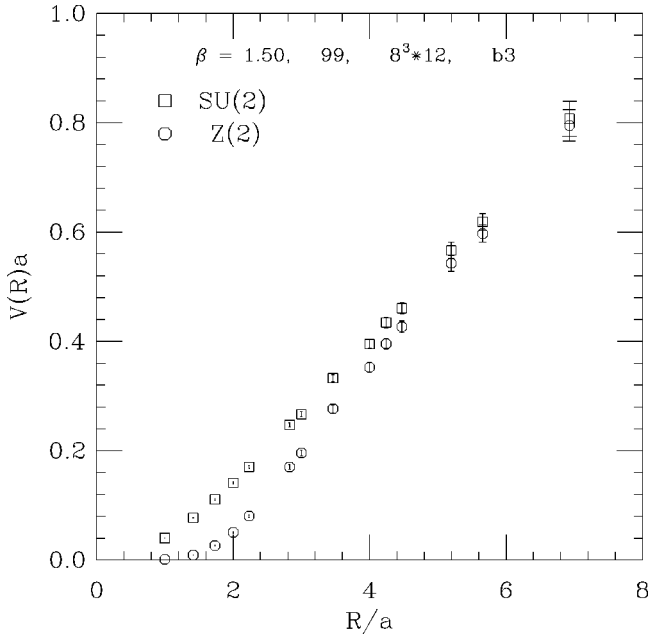

FIG. 11. The same as Fig. 9 but measured after 3 smoothing steps. Squares represent the potential obtained from Wilson loop averages, the octagons are obtained from Wilson loop sign averages.

ing destroyed a significant number of thin vortices and on this short distance scale thin vortices no longer dominate the potential. On the other hand thicker vortices could not be destroyed by a local smoothing and the long-distance features are thus preserved. In this context we note that exactly the same type of behavior would be expected from the positive plaquette model, in which the plaquettes are constrained to be non-negative. This constraint does not allow the formation of thin vortices but vortices thicker than one plaquette are not affected significantly.

Finally we repeated the comparison of the full and the sign potential after an additional two smoothing steps were performed (Fig. 11). As a result of further smoothing the short distance disagreement of the potentials extend to a bit longer distances but the asymptotic string tension is not affected. This is consistent with our expectations that as more and more smoothing is performed, vortices of larger size are also destroyed. For a fixed number of smoothing steps, however, there is always a scale beyond which thick vortices remain intact. Beyond this scale one effectively has the same physical situation as before the smoothing. This may be viewed as being on a fictitious coarser lattice with the lattice spacing set by this scale and with thin and thick vortices relative to this scale. Thus the vortex contribution to the asymptotic string tension is not affected by smoothing.

V. CONCLUSIONS

We presented a picture of the QCD vacuum by identifying the gauge field excitations that can disorder the system on large distance scales and can thus lead to confinement even at weak coupling. The relevant excitations are thick spread-out center vortices that make the sign of large Wilson loops fluctuate considerably. The vortices are extended objects that cost very little in local action but have a long-range disordering effect. As opposed to thin vortices which gradually freeze out when the coupling is lowered, the thick vortices are expected to survive at arbitrarily weak couplings.

We tested numerically how the vortices affect the Wilson loop expectations and the deduced heavy quark potential. In the $SU(2)$ case vortices linking with the Wilson loop are responsible for the fluctuation of its sign. Therefore we compared the heavy-quark potential extracted from full Wilson loops with the potential extracted from the expectation of the sign of Wilson loops. The sign expectation counts the contribution of all types of vortices. The measurements were performed with the Wilson action at two different couplings as well as with a perfect action. In all three cases the two potentials completely agreed even for small distances.

To check the universality of this picture we repeated the same test on an ensemble of locally smoothed configurations. The agreement of the long-distance part of the potentials persisted after the smoothing. This shows that all the relevant long-distance physical properties are encoded in the fluctuation of the sign of the Wilson loops which in turn is governed by the vortices linking with it.

ACKNOWLEDGMENTS

The research of T.K. was supported by DOE grant DE-FG02-92ER-40672. The research of E.T. was supported by NSF grant NSF-PHY 9531023.

[1] G. Mack and V. B. Petkova, Ann. Phys. (N.Y.) **123**, 442 (1979); **125**, 117 (1980); Z. Phys. C **12**, 177 (1982).
[2] L. G. Yaffe, Phys. Rev. D **21**, 1574 (1980).
[3] E. T. Tomboulis, Phys. Rev. D **23**, 2371 (1981); in *Proceedings of the Brown Workshop on Nonperturbative Studies in QCD*, Providence, Rhode Island, 1981, edited by A. Jevicki and C-I. Tan (Brown University Report No. 457, Providence, 1981).
[4] T. Yoneya, Nucl. Phys. **B205 [FS5]**, 130 (1982).
[5] J. M. Cornwall, Phys. Rev. D **26**, 1453 (1982); in *Workshop on Non-perturbative QCD*, Proceedings, Stillwater, Oklahoma, edited by K. A. Milton and M. A. Samuel (Birkhauser, Boston, 1983).
[6] E. T. Tomboulis, Phys. Lett. B **303**, 103 (1993); in *Lattice '93*, Proceedings of the International Symposium, Dallax, Texas, edited by T. Draper *et al.* [Nucl. Phys. B, Proc. Suppl. (Proc. Suppl.) **34**, 192 (1994)]; T. G. Kovács and E. T. Tomboulis, *Lattice '96*, Proceedings of the International Symposium, St. Louis, Missouri, edited by C. Bernard *et al.* [*ibid.* **53**, 509 (1997)]; hep-lat/9709042.
[7] L. Del Debbio, M. Faber, J. Greensite, and S. Olejník, Phys. Rev. D **55**, 2298 (1997); hep-lat/9708023; hep-lat/9709032.
[8] P. Goddard and D. I. Olive, Rep. Prog. Phys. **41**, 91 (1978).
[9] J. Fröhlich, R. Israel, E. H. Lieb, and B. Simon, Commun. Math. Phys. **62**, 1 (1978); D. Brydges, J. Fröhlich, and E. Seiler, Ann. Phys. (N.Y.) **121**, 227 (1979).
[10] G. 't Hooft, Nucl. Phys. **B153**, 141 (1979).
[11] E. T. Tomboulis and L. G. Yaffe, Commun. Math. Phys. **100**, 313 (1985).
[12] U. M. Heller, K. M. Bitar, R. G. Edwards, and A. D. Kennedy, Phys. Lett. B **335**, 71 (1994).
[13] T. G. Kovacs and Z. Schram, Phys. Rev. D **56**, 6824 (1997).
[14] A. Hart, and M. Teper, preprint LSUHE-262-1997; hep-lat/9709009.
[15] T. DeGrand, A. Hasenfratz, and T. G. Kovacs, Nucl. Phys. **B505**, 417 (1997).